

## 7.4: Iron-sulfur Proteins and Models (Part 4)

### Core Extrusion/Cluster Displacement Reactions

Synthetic model-system work led to the realization that the cluster cores can exist outside the protein and undergo relatively facile ligand-exchange reactions.<sup>128</sup> This behavior of the purely inorganic complexes allowed core extrusion reactions<sup>128,144</sup> to be developed. The basic assumption behind these reactions is that the cluster core retains its integrity when it is substituted by low-MW thiolates, especially aryl thiolates, which replace the cysteinyl ligands that bind it to the protein. In order to free the cluster from the protein, one must at least partially denature the protein, usually by using ~80 percent aqueous solution of a polar aprotic solvent, such as DMSO or HMPA. The resulting inorganic clusters can be identified and quantified by measurement of their characteristic electronic absorption or NMR spectra. An alternative approach involves transferal of the unknown cluster in question to an apoprotein that binds a cluster of known type.<sup>145</sup>

Since the 1Fe, 2Fe, and 4Fe sites are each usually bound to the protein by four cysteine residues, it is perhaps not surprising that there have been reports<sup>58</sup> of interconversion of cluster types bound to a given protein. Specifically, in 90 percent aqueous DMSO, the single Fe site in rubredoxin from *C. pasteurianum* is converted to an  $\text{Fe}_4\text{S}_4$  cluster by the addition of sodium sulfide, ferrous chloride, and ferric chloride in ratio 4:2:1. Presumably the spacing and geometric disposition of the cysteines are suitable to bind a single Fe or the  $\text{Fe}_4\text{S}_4$  cluster, which is readily formed under the reaction conditions. Another example of cluster rearrangement involves the three-iron center discussed below that does *not* extrude as an  $\text{Fe}_3\text{S}_4$  center. Rather, at least under *certain* conditions, the  $\text{Fe}_{3\text{Sx}}$  center rearranges to form  $\text{Fe}_2\text{S}_2$  centers.<sup>146</sup> The facile interconversion of the Fe clusters demonstrated the lability of Fe-S systems, and indicates that caution must be exercised in interpreting the results of cluster-displacement reactions.

### $\text{Fe}_3\text{S}_4$ Centers

Three-iron centers are a comparatively recent finding,<sup>119,146</sup> and the full scope of their distribution is not yet known. Although they have now been confirmed in dozens of proteins, it often remains uncertain what physiological role these centers play. Indeed, since  $\text{Fe}_3\text{S}_4$  centers can be produced as an artifact upon oxidation of  $\text{Fe}_4\text{S}_4$  centers, it has been suggested that 3Fe centers may not be truly physiological, and could be side products of aerobic protein isolation. This caveat notwithstanding, the 3Fe sites are being found in more and more proteins and enzymes. Their physiological *raison d'être* may be more subtle than that of their 1, 2, and 4Fe cousins; we should certainly try to find out more about them. Some proteins containing  $\text{Fe}_3\text{S}_4$  centers are listed in Table 7.1.

The 3Fe center was first recognized<sup>147</sup> in the protein ferredoxin I from the anaerobic nitrogen-fixing bacterium *Azotobacter vinelandii*. The protein is called Av FdI for short. It is instructive to sketch historically the evolution of our understanding of this protein. Av ferredoxin I was reported to have 6 to 8 Fe atoms and was first thought to resemble the clostridial 8Fe ferredoxins. However, unlike the clostridial protein, the Av FdI clusters appeared to have two quite different redox couples at +320 and -420 mV. Although it might have been thought that this protein contained one HiPIP-type and one Fd- or "ferredoxin"-type  $\text{Fe}_4\text{S}_4$  cluster, the protein as isolated had an EPR signal with  $g = 2.01$ , which differed significantly (Figure 7.6) from that of an oxidized HiPIP or a reduced Fd.<sup>148</sup> Cluster extrusion reactions also seemed to indicate the presence of an unusual cluster type.<sup>149</sup>

Fortunately, the protein was crystallized, and could be studied by x-ray diffraction. Unfortunately, the initial conclusions<sup>150</sup> and subsequent revisions<sup>151,152</sup> of the crystal-structure analysis have proven to be wrong, teaching us in the process that protein x-ray crystallography, taken alone, does not always provide definitive results. Specifically, the first crystallographic report suggested the presence of a conventional  $\text{Fe}_4\text{S}_4$  cluster and a smaller packet of electron density that was assigned as a 2Fe-2S center.<sup>150</sup> However, upon further refinement, and following the formulation of the 3Fe center by Mössbauer spectroscopy,<sup>147</sup> a 3Fe-3S center was identified and refined.<sup>151,152</sup> The "refined"  $\text{Fe}_3\text{S}_3$  center was a six-membered alternating iron-sulfide ring with an open, almost flat, twistedboat conformation (Figure 7. 14). The Fe-Fe separation of 4.1 Å and the structural type was unprecedented, and did not agree with the results of resonance Raman spectroscopy,<sup>153</sup> with x-ray absorption spectroscopy on the native protein or on samples from which the  $\text{Fe}_4\text{S}_4$  center was removed,<sup>103</sup> or even with stoichiometry, which eventually led to the reformulation<sup>154</sup> of the cluster as  $\text{Fe}_3\text{S}_4$ . The x-ray absorption studies (EXAFS) clearly led to the assignment of a 2.7-Å Fe-Fe distance for the 3Fe cluster.<sup>103</sup>

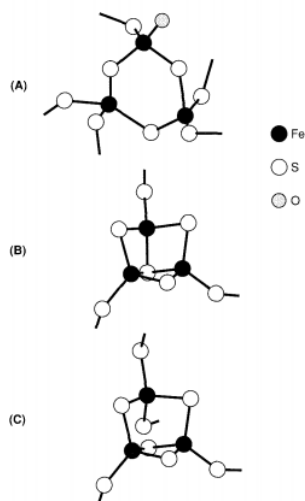


Figure 7.14 -  $\text{Fe}_3\text{S}_n$  structures: (A) open  $\text{Fe}_3\text{S}_3$  structure proposed from initial x-ray studies (now shown to be in error); (B) the thiocubane fragment structure believed present in most  $\text{Fe}_3\text{S}_4$  proteins; (C) open  $\text{Fe}_3\text{S}_4$  structure (not found to date).

In parallel with the studies on Av FdI, two additional proteins played key roles in the resolution of the nature of the  $\text{Fe}_3$  cluster. These are FdII from *Desulfovibrio gigas* and aconitase from beef heart. Each contains (under certain conditions) only  $\text{Fe}_3\text{S}_4$  sites, thus enabling more definitive structural, stoichiometric, and spectral information to be acquired. Studies on these proteins using EXAFS,<sup>155</sup> Mössbauer,<sup>52,156,157</sup> EPR,<sup>146</sup> and resonance Raman (to which we will return briefly) clearly favor the closed structure shown in Figure 7.14C. Indeed, x-ray crystallography on aconitase by the same group that did the initial x-ray work on Av FdII revealed the compact structure in agreement with the spectroscopy.<sup>20</sup>

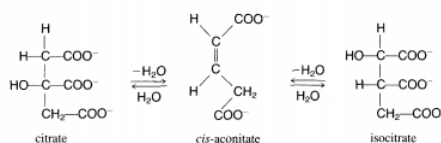
In 1988 the structural error in the crystallography of Av FdI was found by two groups, and a new refinement in a corrected space group led to a structure in agreement with the spectroscopy.<sup>111,112</sup> The  $\text{Fe}_3\text{S}_4$  cluster has the apoFe thiocubane structure, with each iron atom bound to the protein by a single cysteinyl thiolate. Clearly, even x-ray crystallography is potentially fallible, and its findings must be critically integrated with the data from other techniques in arriving at full structural definition of metalloenzyme sites.

The studies on the ferredoxins from *D. gigas* present an interesting lesson on the lability of the Fe-S cluster systems. Two distinct proteins from *D. gigas*, FdI and FdII, contain the same polypeptide chain (6 kDa) in different states of aggregation,<sup>158,159</sup> Whereas FdI is a trimer containing three  $\text{Fe}_4\text{S}_4$  clusters, FdII is a tetramer that contains four  $\text{Fe}_3\text{S}_4$  clusters. The ferredoxins differ in their redox potentials and appear to have different metabolic functions in *D. gigas*. The oxidation of *D. gigas* FdI with  $\text{Fe}(\text{CN})_6^{3-}$  leads to FdII, and treatment of FdII with iron salts leads to FdI. The *D. gigas* system reveals the lability and interconvertibility of Fe-S clusters. The recently reported<sup>160</sup> crystal structure of *D. gigas* FdII shown in Figure 7.15 confirms the partial (apoFe) thiocubane  $\text{Fe}_3\text{S}_4$  center. The iron atoms are ligated by three cysteinyl residues from protein side chains. The cube missing an iron is now firmly established as a viable structural type.



Figure 7.15 - The x-ray crystal structure of *D.gigas* FdII, illustrating the  $\text{Fe}_4\text{S}_4$  and  $\text{Fe}_3\text{S}_4$  centers in this protein.<sup>160</sup>

The aconitase system presents yet another fascinating story.<sup>159a</sup> Aconitase is a key enzyme in the Krebs cycle, catalyzing the conversion of citrate and isocitrate through the intermediacy of cis-aconitate, as shown in Equation (7.6).



(7.6)

This is a hydrolytic nonredox process, and for some time it was thought that aconitase was a simple  $\text{Fe}^{2+}$  protein wherein the ferrous iron was involved in the Lewis-acid function of facilitating the hydrolytic reaction. Indeed, aconitase is inactive when isolated from mitochondria, and requires the addition of  $\text{Fe}^{2+}$  to achieve activity.

Surprisingly, the isolated aconitase was found by analysis and Mossbauer spectroscopy to possess an  $\text{Fe}_3\text{S}_4$  site in its inactive form.<sup>161</sup> Low-resolution crystallographic study supports the presence of an apo-Fe thiocubane,  $\text{Fe}_3\text{S}_4$  structure in aconitase.<sup>162</sup> Resonance Raman<sup>163</sup> and EXAFS<sup>103,155</sup> studies clearly fingerprint the  $\text{Fe}_3\text{S}_4$  cluster. The current hypothesis for aconitase activation involves the  $\text{Fe}_3\text{S}_4$  thiocubane fragment reacting with  $\text{Fe}^{2+}$  to complete the cube, which is the active form of the enzyme.<sup>164</sup> Recent crystallographic studies<sup>113</sup> confirm the presence of a complete cube in the activated aconitase. The dimensions and positioning of the  $\text{Fe}_3\text{S}_4$  and  $\text{Fe}_4\text{S}_4$  centers in the cube are virtually identical. The added  $\text{Fe}^{2+}$  iron atom is ligated by a water (or hydroxide) ligand, consistent with the absence of any cysteine residues near the exchangeable iron. Since this water (or a hydroxide) is also present in the  $\text{Fe}_3\text{S}_4$  system, one wonders whether a small ion such as  $\text{Na}^+$  might be present in the  $\text{Fe}_3\text{S}_4$  aconitase system.

Questions of detailed mechanism for aconitase remain open. ENDOR spectroscopy<sup>165</sup> shows that both substrate and water (or  $\text{OH}^-$ ) can bind at the cluster. Does one of its Fe-atom vertices play the Lewis-acid role necessary for aconitase activity? Is the  $\text{Fe}_3\text{S}_4 \rightleftharpoons \text{Fe}_4\text{S}_4$  conversion a redox- or iron-activated switch, which works as a control system for the activity of aconitase? These and other questions will continue to be asked. If aconitase is indeed an Fe-S enzyme with an iron-triggered control mechanism, it may be representative of a large class of  $\text{Fe}_3/\text{Fe}_4$  proteins. Other hydrolytic enzymes containing similar Fe-S centers have recently been reported.<sup>166,166a</sup>

Spectroscopically, the  $\text{Fe}_3\text{S}_4$  center is distinct and clearly distinguishable from 1Fe, 2Fe, and 4Fe centers. The center is EPR-active in its oxidized form, displaying a signal (Figure 7.6) with  $g = 1.97, 2.00, \text{ and } 2.06$  (*D. gigas* FdII).<sup>158</sup> The Mössbauer spectrum (Figure 7.7) shows a single quadrupole doublet with  $\Delta Q = 0.53 \text{ nm/s}$  and isomer shift of  $0.27 \text{ nm}$ , suggesting the now familiar highspin iron electronic structure.<sup>158,159</sup> In its reduced form, the center becomes EPR-silent, but the Mössbauer spectrum now reveals two quadrupole doublets of intensity ratio 2:1. The suggestion of the presence of a 3Fe center was first made based on this observation.<sup>147</sup> The picture of the reduced  $\text{Fe}_3\text{S}_4$  state that has emerged involves a coupled, delocalized  $\text{Fe}^{2+}/\text{Fe}^{3+}$  unit responsible for the outer doublet, with a single  $\text{Fe}^{3+}$  unit responsible for the inner doublet of half the intensity. The oxidized state contains all  $\text{Fe}^{3+}$  ions, which are coupled in the trinuclear center.

EXAFS studies were consistent and unequivocal in finding an Fe-Fe distance of  $\sim 2.7 \text{ \AA}$  in all putative  $\text{Fe}_3\text{S}_4$  proteins.<sup>103,155,167</sup> Resonance Raman spectra compared with those of other proteins and of model compounds with known structures<sup>168,169</sup> for other metals also favored the structure of Figure 7.14B. Clearly, what has been termed the spectroscopic imperative<sup>170</sup> has been crucial in the successful elucidation of the 3Fe structure. An interesting excursion has led to isolation of what are presumed to be  $\text{ZnFe}_3\text{S}_4$ ,  $\text{CoFe}_3\text{S}_4$ , and  $\text{NiFe}_3\text{S}_4$  thiocubane structures by adding  $\text{Zn}^{2+}$ ,  $\text{Co}^{2+}$ , or  $\text{Ni}^{2+}$ , respectively, to proteins containing reduced  $\text{Fe}_3\text{S}_4$  cores.<sup>170a,b,c</sup> These modified proteins provide interesting electronic structural insights and, potentially, new catalytic capabilities.

## Fe<sub>3</sub> Model Systems

To date, the  $\text{Fe}_3\text{S}_4$  center is the only structurally characterized biological iron-sulfide center that does not have an analogue in synthetic Fe chemistry. In fact, the closest structural analogue<sup>21,170d</sup> is found in the  $\text{Mo}_3\text{S}_4^{4+}$  or  $\text{V}_3\text{S}_4^{3+}$  core in clusters such as  $\text{Mo}_3\text{S}_4(\text{SCH}_2\text{CH}_2\text{S})_3^{2-}$ , whose structure is shown in Figure 7.16.

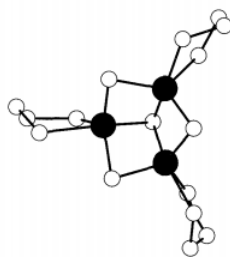


Figure 7.16 - The x-ray crystal structure of  $\text{Mo}_3\text{S}_4(\text{SCH}_2\text{CH}_2\text{S})_3^{2-}$ . (From Reference 10a.)

The resonance Raman spectrum<sup>169</sup> of this complex bears a close resemblance to that of the *D. gigas* ferredoxin II. Since the vibrational bands responsible for the resonance Raman spectrum are not strongly dependent on the electronic properties, it is not surprising that an analogue with a different metal can be identified using this technique.

In synthetic Fe chemistry, although there is no precise structural analogue, it is instructive to consider three types of trinuclear and one hexanuclear center in relation to the three-iron biocenter.

The trinuclear cluster  $\text{Fe}_3\text{S}[(\text{SCH}_2)\text{C}_6\text{H}_4]_3^{2-}$  is prepared<sup>171,172</sup> by the reaction of  $\text{FeCl}_3$ ,  $\text{C}_6\text{H}_4(\text{CH}_2\text{SH})_2$ ,  $\text{Na}^+\text{OCH}_3^-$ , and *p*- $\text{CH}_3\text{-C}_6\text{H}_4\text{-SH}$  in  $\text{CH}_3\text{OH}$ . As shown in Figure 7.17A, this cluster has, like the biocluster, a single triply bridging sulfide ion but, unlike the biocluster, it uses the sulfur atoms of the ethane 1,2-dithiolate as doubly bridging, as well as terminal, groups. The inorganic ring  $\text{Fe}_3(\text{SR})_3\text{S}_6^{3-}$  ( $\text{X} = \text{Cl}, \text{Br}$ ) has a planar  $\text{Fe}_3(\text{SR})_3$  core, which resembles the now-discredited structure for Av FdI<sup>173</sup> (Figure 7.14A).

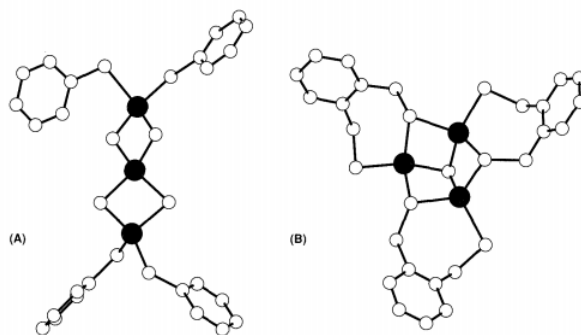


Figure 7.17 - The x-ray crystal structures of trinuclear Fe complexes: (A)  $\text{Fe}_3\text{S}_4(\text{SR})_4^{3-}$ ; (B)  $\text{Fe}_3\text{S}[(\text{SCH}_2)_2\text{C}_6\text{H}_4]_3^{2-}$ . (Data from References 171, 172, 174, 175.)

The complex  $\text{Fe}_3\text{S}_4(\text{SR})_4^{3-}$  is prepared<sup>174,175</sup> by reaction of  $\text{Fe}(\text{SR})_4^{2-}$  with sulfur. The x-ray-determined structure reveals two tetrahedra sharing a vertex with the linear Fe-Fe-Fe array shown in Figure 7.17B. This complex has distinctive EPR, Mössbauer, and NMR spectra that allow it to be readily identified<sup>174,175,175a</sup>. Interestingly, after the complex was reported, a study of (denatured) aconitase at high pH (>9.5) revealed that the thiocubane fragment  $\text{Fe}_3\text{S}_4$  site in that enzyme rearranged to adopt a structure that was spectroscopically almost identical with that of the linear complex.<sup>176</sup> Although the state may not have any physiological significance, it does show that Fe-S clusters different from the common (conventional) ones already discussed could be important in proteins under certain physiological conditions or in certain organisms; i.e., iron centers first identified synthetically may yet prove to be present in biological systems.

A synthetic cluster that displays features related to the biological  $\text{Fe}_3\text{S}_4$  cluster is the hexanuclear cluster  $\text{Fe}_6\text{S}_9(\text{SR})_2^{4-}$  shown in Figure 7.18. This cluster contains two  $\text{Fe}_3\text{S}_4$  units bridged through their diiron edges by a unique quadruply bridging  $\text{S}^{2-}$  ion ( $\mu_4\text{-S}^{2-}$ ) and by two additional  $\mu_2\text{S}^{2-}$  bridges. The inability of synthetic chemists to isolate an  $\text{Fe}_3\text{S}_4$  analogue may indicate that in proteins this unit requires strong binding. Significant sequestration by the protein may be needed to stabilize the  $\text{Fe}_3\text{S}_4$  unit against oligomerization through sulfide bridges or, alternatively, rearrangement to the stable  $\text{Fe}_4\text{S}_4$  center.

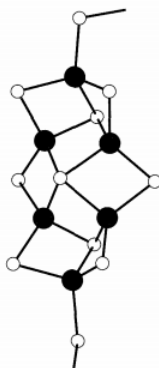


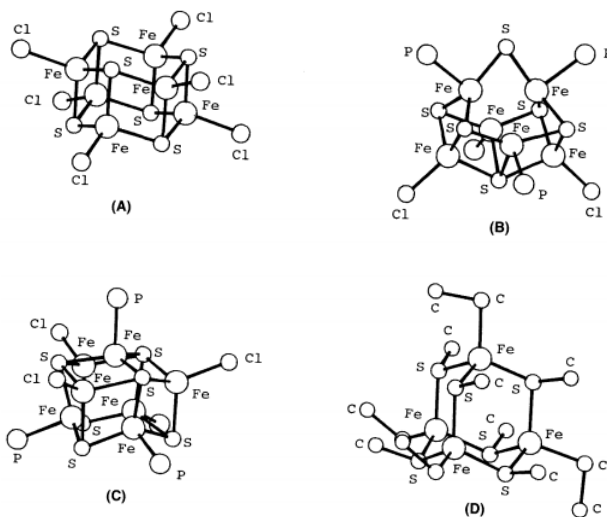
Figure 7.18 - The x-ray crystal structure<sup>176a,b</sup> of  $\text{Fe}_6\text{S}_9(\text{SR})_2^{4-}$ .

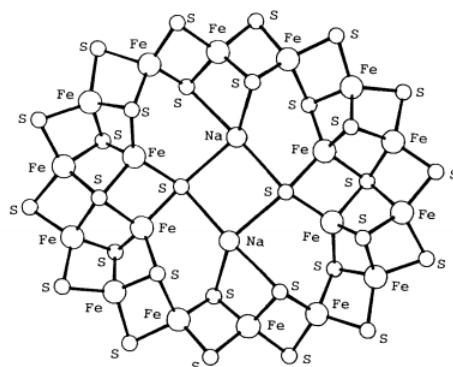
## Fe-S Chemistry: Comments and New Structures

The first successful model system for an iron-sulfur protein was an analogue of the  $\text{Fe}_4\text{S}_4$  system, i.e., the system with the largest presently established biological Fe cluster. The reactions used to synthesize the cluster shown in Figure 7.13 are said to involve self-assembly, meaning that starting materials are simply mixed together, and thermodynamic control causes the cluster to assemble in its stable form. Interestingly, the  $\text{Fe}_4\text{S}_4$ -containing proteins, such as those of *C. pasteurianum*, are considered to be among the most ancient of proteins. Perhaps on the anaerobic primordial Earth, Fe-S clusters self-assembled in the presence of protein ligands to form the progenitors of the modern ferredoxins.

Much progress has been made in synthetic chemistry, and it is clear that both understanding and control of Fe-S chemistry are continuing to grow. New preparations for known clusters continue to be found, and new clusters continue to be synthesized. Although many of the new clusters appear to be abiological, we should not ignore them or their potential. They add to our understanding of Fe-S chemistry in general, and serve as starting points in the study of heteronuclear clusters. There is also the distinct possibility that one or more of these synthetic clusters represent an existing biological site that has not yet been identified in an isolated system.

Among the "nonbiological" structures that have been synthesized are complexes with  $\text{Fe}_6\text{S}_6^{3+/2+}$  cores<sup>177,178</sup> including the thioprismanes,<sup>108,109,177-179</sup> the octahedron/cube  $\text{Fe}_6\text{S}_8^{3+}$  cores,<sup>180,181</sup> the  $\text{Fe}_6\text{S}_9^{2-}$  cores<sup>176a,b</sup> discussed above, the adamantane-like  $\text{Fe}_6(\text{SR})_{10}^{4-}$  complexes related to Zn and Cu structures in metallothioneins,<sup>182</sup> basket  $\text{Fe}_6\text{S}_6^{2+}/\text{Fe}_6\text{S}_6^+$  cores,<sup>182a,b,c,d</sup> monocapped prismatic  $\text{Fe}_7\text{S}_6^{3+}$  cores,<sup>183</sup> the cube/octahedron  $\text{Fe}_8\text{S}_6^{5+}$  cores,<sup>179</sup> and the circular  $\text{Na}^+$ -binding  $\text{Fe}_{18}\text{S}_{30}^{10-}$  unit.<sup>183a,b</sup> Representative ions are shown in Figure 7.19. Some of these cores are stabilized by distinctly nonbiological phosphine ligands. Nevertheless, one should not *a priori* eliminate any of these structures from a possible biological presence. Indeed, recently a novel, apparently six-iron protein from *Desulfovibrio gigas* has been suggested<sup>183c</sup> to have the thioprismane core structure first found in model compounds.





(E)

Figure 7.19 - Structures of "to date nonbiological" Fe-S clusters: (A) the thioprismane structure;<sup>177</sup> (B) basket-handle structure;<sup>182a</sup> (C) monocapped prismatic structure;<sup>183</sup> (D) adamantane structure;<sup>182</sup> (E) circular  $\text{Fe}_{18}\text{S}_{30}^{10-}$  core unit.<sup>183a,b</sup>

## Detection of Fe-S Sites

Several recent reviews have concentrated on the ways in which the various Fe-S centers can be identified in newly isolated proteins.<sup>5,6,184</sup> It is instructive to summarize the central techniques used in the identification of active sites. Optical spectra are usually quite distinctive, but they are broad and of relatively low intensity, and can be obscured or uninterpretable in complex systems. MCD spectra can give useful electronic information, especially when the temperature dependence is measured. EPR spectra, when they are observed, are distinctive, and are usually sufficiently sharp to be useful even in complex systems. Mössbauer and resonance Raman spectroscopies have each been applied with good effect when they can be deconvoluted, and NMR and magnetic susceptibility have given important information in some simple, lower-MW protein systems. X-ray absorption spectra, especially EXAFS, give accurate Fe-S and Fe-Fe distances when a single type of Fe atom is present. Analytical and extrusion data complement the spectroscopic and magnetic information. Extrusion data must be viewed with considerable caution, because of possible cluster-rearrangement reactions. Even x-ray crystallography has led to incorrect or poorly refined structures. In general, no one technique can unequivocally identify a site except in the very simplest systems, and there is continued need for synergistic and collaborative application of complementary techniques to a given system.

## Redox Behavior

Figure 7.20 shows the ranges of redox behavior known for Fe-S centers. Clearly, the Fe-S systems can carry out low-potential processes. The rubredoxins cover the mid-potential range, and the HiPIPs are active in the high-potential region. The lack of extensive Fe-S proteins in the positive potential region may reflect their instability under oxidizing conditions and their preemption by Mn, Cu, or heme-iron sites (such as in cytochrome c), which function in this region.

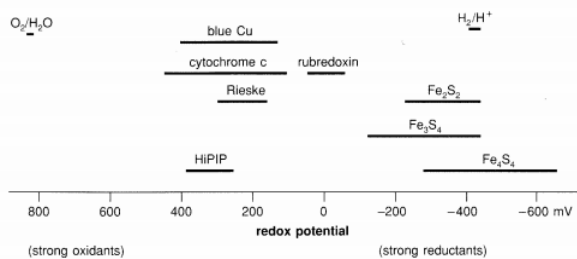


Figure 7.20 - A schematic diagram of the redox potential of the various FeS centers in comparison with other known redox centers.

7.4: Iron-sulfur Proteins and Models (Part 4) is shared under a [CC BY-NC-SA 4.0](https://creativecommons.org/licenses/by-nc-sa/4.0/) license and was authored, remixed, and/or curated by LibreTexts.